

proach in this quest. First, note that the extensive biaxial phase region on the right side of Fig. 1 corresponds to high density and/or low temperature. Experience with ordinary nematic liquid crystals indicates that these conditions are likely to lead to crystallization before a biaxial phase could appear. However, according to Fig. 1, it should also be possible to reach the biaxial phase by adjusting  $T^*$ , the effective molecular asymmetry parameter, without necessarily decreasing the range of stability of the liquid crystal phases or changing conditions likely to affect crystallization. The biaxial phase and the special critical behavior should both appear when we achieve a crossover between rodlike and plate-like behavior. One way to do this would be to make mixtures of rodlike and platelike molecules<sup>8</sup> with similar melting points and favorable dispersion interactions.<sup>9</sup> The phase diagram for such a two-component fluid would be similar to that in Fig. 1 with concentration playing the role of  $T^*$ . Furthermore, such a mixture would ameliorate the ever-present chance that crystallization might intervene before a biaxial phase could be achieved. Even before a biaxial phase appears, the onset of the crossover region might be investigated by measuring the behavior in the discontinuity in the order parameter  $\nu$  at the isotropic-uniaxial transition and looking for a linear decrease as the point  $A$  is approached.

In conclusion, we have solved a model in a mean-field approximation, and the results suggest that a fluid of biaxial particles might be a most interesting system for both theoretical and experimental study of phase transitions.

It is a pleasure to acknowledge helpful discussions with James McColl, Michael Fisher, Joseph Straley, Denis Weaire, and W. P. Wolf.

---

\*Work supported in part by the U. S. Army Research Office (Durham) under Grant No. DA-ARO-D-31-124-72-G169, and by the Office of Naval Research under Contract No. N00014-67-A-0097-0013.

<sup>1</sup>R. B. Griffiths, *Phys. Rev. Lett.* **24**, 1479 (1970).

<sup>2</sup>R. B. Griffiths, *Phys. Rev. Lett.* **24**, 715 (1970).

<sup>3</sup>In this we exclude the well known smectic- $C$  phase whose biaxial symmetry is intimately connected with the presence of two-dimensional positional order. See T. R. Taylor, J. L. Fergason, and S. L. Arora, *Phys. Rev. Lett.* **24**, 359 (1970).

<sup>4</sup>M. J. Freiser, *Phys. Rev. Lett.* **24**, 1041 (1970).

<sup>5</sup>C. S. Shih and R. Alben, *J. Chem. Phys.* **57**, 3057 (1972).

<sup>6</sup>It should be noted that even "ordinary" critical behavior would be quite extraordinary for liquid crystals since truly critical phase transitions have never been observed in these systems.

<sup>7</sup>P. J. Flory, *J. Chem. Phys.* **12**, 425 (1944), and *Proc. Roy. Soc., Ser. A* **234**, 60, 73 (1950).

<sup>8</sup>J. F. Dreyer, *J. Phys. (Paris)* **30**, C4-114 (1969).

<sup>9</sup>R. Alben, unpublished.

---

## Neutron-Scattering Observations of Critical Slowing Down of an Ising System

M. R. Collins and H. C. Teh

*Physics Department, McMaster University, Hamilton, Ontario, Canada*

(Received 30 January 1973)

We have studied the dynamics of the order-disorder phase transition in  $Ni_3Mn$  by neutron-scattering techniques. The relaxation time constant for the long-range order is about 90 min at a temperature  $15^\circ\text{C}$  below the critical temperature, but closer to the critical temperature it increases by more than an order of magnitude. This critical slowing down varies as the reduced temperature to a power of  $1.04 \pm 0.09$ .

The full dynamic behavior of Ising systems is not built into the Hamiltonian since the Hamiltonian does not provide a mechanism for changing the  $z$  component of spin on any atom. A number of recent theoretical treatments<sup>1-6</sup> have introduced an external spin-flipping mechanism to bring the system to equilibrium and, on this basis, have predicted critical slowing down with a time constant given by the reduced temperature

raised to some power.

Order-disorder critical phase transitions in binary alloys are believed to be excellent examples of Ising-type phase transitions.<sup>7,8</sup> The Hamiltonian for the alloy ordering process is equivalent to the Ising Hamiltonian if it is assumed that the ordering energy varies linearly with the number of neighbors of a given type. The mechanism which actually moves the atoms from one lattice

site to another in the ordering process will be of a diffusion type, probably vacancy diffusion in the case we consider.

We chose the order-disorder process in  $\text{Ni}_3\text{Mn}$  for the present investigation for five reasons. Firstly, it seemed that the time constants involved were likely to be of order of a few hours, and this is experimentally convenient. Secondly, manganese and nickel atoms have similar size so the order-disorder process should not involve long-range strains, and it is hoped that the Hamiltonian corresponds closely to an Ising model with short-range interactions. Thirdly, the neutron cross sections were specially favorable for such measurements because of the negative scattering length of manganese; fourthly, large single crystals were available; and fifthly, the transition has been shown to be of a critical type.<sup>9</sup>

The specimen was a single crystal of  $\text{Ni}_2\text{Mn}$  grown by the Czochralski method and purchased from Materials Research Corporation, Orangeburg, N. Y. The crystal was in the form of a cylinder 1 in. long,  $\frac{1}{2}$  in. in diameter, mounted about  $15^\circ$  from the vertical. The uniformity of the critical temperature through the specimen to within  $0.5^\circ$  indicates that the chemical composition was uniform to about 0.05% throughout the crystal.<sup>10</sup>

The crystal was mounted in a vacuum furnace that had a temperature stability of about  $0.2^\circ\text{C}$  over long periods. The temperature gradient across the specimen was also about  $0.2^\circ\text{C}$ . The response time of the furnace was such that it was possible to give the specimen a step-like change in temperature of a few degrees over a period of about 5 min without inducing specimen temperature oscillations. This time was more than an order of magnitude faster than the response time of the order-disorder system.

The degree of long-range order in the system was measured by observing the intensity of the (100) superlattice Bragg peak on a conventional neutron double-axis spectrometer set for a neutron wavelength of  $1.05 \text{ \AA}$ . The spectrometer was located at the McMaster University reactor. Although the (100) Bragg peak was less intense than the (200) peak by a factor of 4 in the ordered state, it is likely that the peak intensity shows some extinction effects. However, it is unlikely that these effects will change so rapidly with temperature as to significantly affect the measured time constants. Relaxed collimation was used and our results should not be affected by domain size effects.

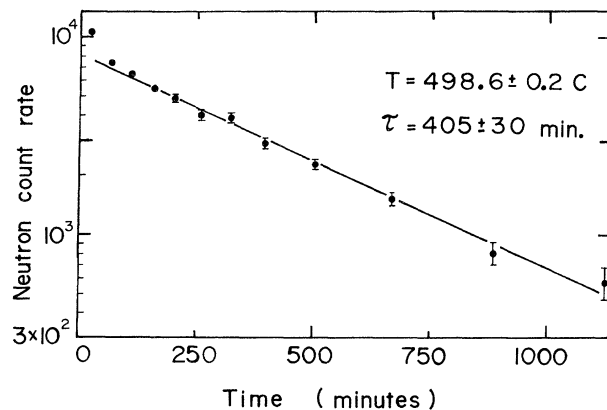


FIG. 1. Semilog plot of the neutron count rate versus time. At time zero, the specimen temperature was changed from  $492$  to  $498^\circ\text{C}$ . The long-range order, as reflected by the neutron count rate, relaxes with a time constant of  $405 \pm 30$  min. The count rate plotted is the difference between the observed rate at a given time and the rate at time  $t = \infty$ .

A typical experimental result is shown in Fig. 1. For this measurement the specimen was held at  $492.0^\circ\text{C}$  until it came to equilibrium and then at time  $t=0$  it was rapidly heated to  $498.6^\circ\text{C}$ . The logarithm of the difference between the count rate at time  $t$  and at time  $t = \infty$  is plotted against  $t$ . For an exponential decay the graph should be a straight line, and this is indeed the case. The slope of the graph gives the time constant  $\tau$ . The results were found to be repeatable and independent of the initial temperature so long as the temperature difference was not too large. For larger temperature differences the points at small times  $t$  departed from the straight-line plot, but the data at larger times followed the linear plot. For reasons which we do not understand, the data did not show the same behavior if the specimen was not allowed to come to (or near to) an equilibrium state before changing the temperature at  $t=0$ .

Figure 2 plots the observed time constants against the temperature  $T$ . The critical slowing down around the critical temperature is quite pronounced, amounting to an order-of-magnitude variation in the time constant. The critical temperature as determined from the peak in Fig. 2 is  $499.7 \pm 0.4^\circ\text{C}$ . There may be some broadening of this temperature by about  $0.5^\circ\text{C}$ . Since our temperature control is a little better than this ( $0.2^\circ\text{C}$ ), it is likely that the broadening indicates small variations in stoichiometry of the specimen.

In interpreting these data we have assumed that the observed time constant  $\tau$  is the product of the

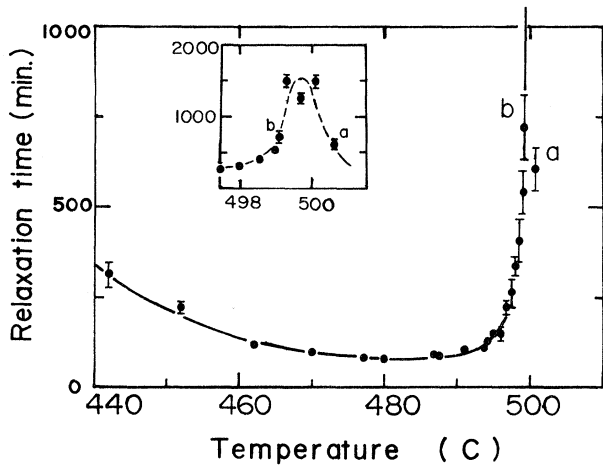


FIG. 2. Relaxation time of the long-range order plotted as a function of temperature. There is a sharp peak at the critical temperature, shown on an expanded temperature scale (inset). The slow increase in the relaxation time at low temperatures arises from the temperature variation of the diffusion process.

Ising time constant  $\tau_I$  and of the diffusion time constant  $\tau_D$ , so that

$$\tau = \tau_I \tau_D. \tag{1}$$

The diffusion time constant can be pictured as setting the unit of time for the operation of the Ising time constant. Over a restricted temperature range the diffusion time is assumed to vary with temperature as

$$\tau_D = A e^{E/kT}, \tag{2}$$

where  $k$  is Boltzmann's constant and  $E$  is the activation energy for the dominant diffusion process.

The Ising time has been assumed to vary with temperature according to a simple power law,

$$\tau_I = B(T_c - T)^{-\Delta}. \tag{3}$$

Equations (1)–(3) have been fitted by least squares to the data of Fig. 2. A satisfactory fit is obtained with or without allowing  $T_c$  to vary. The best fit gave  $T_c = 500.0 \pm 0.3^\circ\text{C}$  and  $E = 3.0 \pm 0.2$  eV. Putting in these values, Fig. 3 shows the Ising time constant  $\tau_I$  plotted against  $1 - T/T_c$  on a log-log scale. The graph forms an excellent straight line with critical exponent  $\Delta = 1.04 \pm 0.09$ .

The theoretical treatments<sup>1-6</sup> of the Ising dynamics concentrate mainly on the two-dimensional case. There the different treatments give values of  $\Delta$  in the range 1.75 to 2, with some conjectures that  $\Delta = \gamma = 1.75$ . Yahata<sup>4</sup> suggests  $\Delta \approx 1.4$  for three dimensions. Both this and a value of  $\Delta$  equal to  $\gamma$  in three dimensions (1.25) are not in

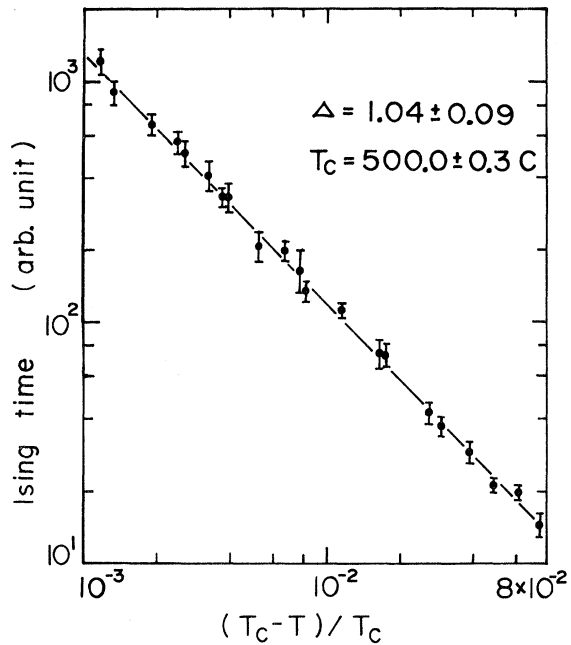


FIG. 3. Log-log plot of the Ising relaxation time versus the reduced temperature. Over two decades of temperatures, there is a straight-line fit corresponding to a critical index of  $1.04 \pm 0.09$ .

accord with our experimental results.

The only other quantitative dynamic data that we have been able to find in the literature for temperatures near enough to  $T_c$  for the critical slowing-down to be seen are those of Siegel<sup>11</sup> and Lord<sup>12</sup> in  $\text{Cu}_3\text{Au}$ . For this material, Cowley<sup>13</sup> has suggested that the phase transition may be of first order, though Lord and Siegel's data are of a type typical of second-order phase transitions.

Lord and Siegel's data were taken before the enormous developments in our understanding of critical transitions during the last 15 years. No quantitative interpretation of their results was attempted. We have fitted Lord's time constant  $\bar{\tau}$  with the equations of this paper. There is a reasonable fit with a critical exponent of 1.18 using  $T_c$  as given by Lord, but a noticeably better fit for a critical temperature 1.6 K lower with critical index 0.81.

It is hoped that this paper will open a new area for study in critical dynamics. There is clearly much more to be done before the complete picture unrolls. Obvious extensions of the work are to measurements above  $T_c$  and to measurements at nonzero wave vector, and also to measurements with other techniques.

We wish to thank Dr. B. N. Brockhouse for the

use of his double-axis neutron spectrometer. We also wish to thank Mr. S. Boronkay, Mr. G. Griffin, and Mr. J. Khatamian for their experimental assistance. This work has been supported financially by the National Research Council of Canada and by the Alfred P. Sloan Foundation.

<sup>1</sup>N. Ogita, A. Veda, T. Matsubara, H. Matsuda, and F. Yonezawa, *J. Phys. Soc. Jap.*, Suppl. **26**, 145 (1969).

<sup>2</sup>H. Yahata and M. Suzuki, *J. Phys. Soc. Jap.* **27**, 1421 (1969).

<sup>3</sup>M. Suzuki, *Progr. Theor. Phys.* **43**, 882 (1970).

<sup>4</sup>H. Yahata, *J. Phys. Soc. Jap.* **30**, 659 (1971).

<sup>5</sup>E. Stoll and T. Schneider, *Phys. Rev. A* **6**, 429 (1972).

<sup>6</sup>T. Schneider, E. Stoll, and K. Binder, *Phys. Rev. Lett.* **29**, 1080 (1972).

<sup>7</sup>J. C. Noovell and J. Als-Nielsen, *Phys. Rev. B* **2**, 277 (1970).

<sup>8</sup>D. R. Chipman and C. B. Walker, *Phys. Rev. Lett.* **26**, 233 (1971).

<sup>9</sup>M. J. Marcinkowski and N. Brown, *J. Appl. Phys.* **32**, 375 (1961).

<sup>10</sup>M. Hansen, *Constitution of Binary Alloys* (McGraw Hill, New York, 1958).

<sup>11</sup>S. Siegel, *J. Chem. Phys.* **8**, 860 (1940).

<sup>12</sup>N. W. Lord, *J. Chem. Phys.* **21**, 692 (1953).

<sup>13</sup>J. M. Cowley, *J. Appl. Phys.* **21**, 24 (1950).

## Energy Bands for $2H\text{-NbSe}_2$ and $2H\text{-MoS}_2$

L. F. Mattheiss

*Bell Telephone Laboratories, Murray Hill, New Jersey 07974*

(Received 16 March 1973)

First-principles calculations of the electronic band structure for the layer-type compounds  $2H\text{-NbSe}_2$  and  $2H\text{-MoS}_2$  predict a 1-eV hybridization gap within the  $d_{z^2}$  and  $d_{xy}$ ,  $d_{x^2-y^2}$  manifolds of the metal-atom  $4d$  bands. This produces a narrow ( $\sim 1$  eV) filled valence band in  $2H\text{-MoS}_2$  and a half-filled conduction band in  $2H\text{-NbSe}_2$ , in agreement with electrical, optical, and recent photoemission data.

There has been considerable interest recently in the electronic structure of the transition-metal dichalcogenide ( $MCh_2$ ) layer compounds. These rather remarkable materials consist of two-dimensional  $ChMCh$  sandwiches that are weakly bonded to one another along the third dimension. This produces highly anisotropic crystals that are readily cleaved and easily intercalated with organic molecules or alkali-metal atoms.<sup>1</sup>

Recent photoemission (PE) studies<sup>2-6</sup> on metallic  $2H\text{-NbSe}_2$  and semiconducting  $2H\text{-MoS}_2$  samples suggest a band-structure model that disagrees with that obtained from a semiempirical tight-binding calculation for  $2H\text{-MoS}_2$  by Bromley, Murray, and Yoffe<sup>7</sup> as well as the more schematic band models of Goodenough,<sup>8</sup> Wilson and Yoffe,<sup>1</sup> and Huisman *et al.*<sup>9</sup> In this Letter, we report the results of first-principles augmented-plane-wave (APW) calculations of the electronic band structures for  $2H\text{-NbSe}_2$  and  $2H\text{-MoS}_2$  which are consistent with the PE, optical, and electrical data. A significant feature of these results is the occurrence of a 1-eV hybridization gap within the M-atom  $4d$  manifold. These results suggest that  $2H\text{-MoS}_2$  and related group-VIB compounds form a

new class of materials in which a hybridization gap is responsible for the observed semiconducting behavior.

The present calculations utilize no empirical data other than the space-group symmetry and the appropriate lattice parameters.<sup>1</sup> They involve approximate crystal potentials that are derived from neutral-atom charge densities, using techniques that have been described previously.<sup>10a</sup>

The results of the present APW calculations are shown in Fig. 1, where  $E(\vec{k})$  curves for both compounds are plotted along symmetry lines in the  $\Gamma MK$  plane as well as the  $\Gamma A$  direction of the hexagonal Brillouin zone. The band shapes are only approximate since the APW calculations have been carried out only at the symmetry points and at the midpoints of the  $\Sigma$  and  $T$  lines. These compounds have similar but not identical crystal structures. Since these  $2H\text{-MCh}_2$  polytypes contain two molecules per cell, there are a total of ten M-atom  $d$  bands and twelve Ch-atom  $p$  bands.

Although covalency effects produce substantial  $p$ - $d$  mixing, the ten bands in the upper portions of Fig. 1 are derived primarily from the metal  $4d$  orbitals, whereas the twelve lower bands originate from the Ch-atom  $p$  orbitals. Covalency ef-